Infrared Physics & Technology 52 (2009) 281–284

Contents lists available at ScienceDirect

Infrared Physics & Technology

journal homepage: www.elsevier.com/locate/infrared

Confinement-enhanced dots-in-a-well QDIPs with operating temperature over 200 K

H.S. Ling [a,*], S.Y. Wang [b], C.P. Lee [a], M.C. Lo [a]

[a] Department of Electronics Engineering, National Chiao Tung University, 1001 Ta Hsueh Road, Hsinchu 300, Taiwan
[b] Institute of Astronomy and Astrophysics, Academia Sinica, P.O. Box 23-141, Taipei, Taiwan

ARTICLE INFO

Article history:
Available online 6 June 2009

PACS:
85.60.Gz
73.50.Pz

Keywords:
Quantum dot
Infrared detector
Photodetector
Intersubband
DWELL
LWIR

ABSTRACT

LWIR InAs/$Al_{0.3}Ga_{0.7}As$/$In_{0.15}Ga_{0.85}As$ confinement-enhanced DWELL (CE-DWELL) QDIPs with operation temperatures higher than 200 K are reported. A thin $Al_{0.3}Ga_{0.7}As$ barrier layer was inserted above the InAs QDs to improve the confinement of QD states in the $In_{0.15}Ga_{0.85}As$ DWELL structure and the device performance. The better confinement of the electronic states increases the oscillator strength of the infrared absorption. The higher excited state energy also improves the escape probability of the photoelectrons. Compared with the conventional DWELL QDIPs, the quantum efficiency increases for more than 20 times and the detectivity is an order of magnitude higher at 77 K. With better device parameters of CE-DWELL, it is possible to achieve high quantum efficiency, high operating temperature and long wavelength detection at the same time.

© 2009 Elsevier B.V. All rights reserved.

1. Introduction

Long wavelength infrared (LWIR, 8–12 μm) detectors are essential to the thermal radiation detection of room temperature objects. With such long detection wavelengths, traditional high quality detectors require low operating temperature which is undesirable from commercial point of view. Quantum dot infrared photodetectors (QDIPs) utilizing intersubband transitions inside quantum dots (QDs) are widely known to be of great potential for the thermal imaging with high operation temperature. The three dimensional carrier confinement of the QD induces the phonon bottleneck which suppresses the interaction between electrons and phonons [1]. With low defect S-K growth mode QDs, several encouraging results have been demonstrated with operation temperatures over 200 K [2,3] and even up to room temperature [4,5]. However, the detection wavelengths of these devices are out of the LWIR atmospheric transmission window.

In order to fit the detection band into the LWIR window, many efforts have been focused on the dots-in-a-well (DWELL) structure [6–10]. The additional quantum well relaxes the limitation due to the QD formation process and provides the possibility to tailor the detection wavelength. More than that, the QDIPs made with the DWELL structures have an additional advantage of lower dark current because the ground state energy is usually lower. In particular, 640 × 512 large format LWIR DWELL QDIP focal plane arrays have been demonstrated recently [11]. Nevertheless, conventional DWELL QDIPs suffer from their inherently lower quantum efficiency. This is a primary drawback since the poor quantum efficiency of QDIPs has always been a concern during the development of the device. With the introduced InGaAs quantum well, the excited state wavefunction spreads out to the well region so that the oscillator strength of the infrared response is reduced. Besides, the photoexcited electrons in the DWELL QDIPs have lower energy relative to the GaAs barrier, making the extraction of photoelectrons more difficult.

In order to solve these problems, in this paper, we propose a modified DWELL structure to enhance both the oscillator strength and the escape probability of the electrons. A thin $Al_{0.3}Ga_{0.7}As$ layer is inserted on top of the InAs QDs in the DWELL structure to provide better confinement for the excited state wavefunction in the QD region and also elevates the excited state energy. The overall quantum efficiency is therefore improved. Furthermore, two samples with different thicknesses of the AlGaAs insertion layers were further compared at different temperatures. Despite the dramatic difference in the device characteristics, both confinement-enhanced DWELL QDIPs can be operated at temperatures higher than 200 K with peak wavelengths at around 8 μm. Thick AlGaAs layers can elevate the dark current activation energy so that the device, although unfavorable for low temperature

* Corresponding author. Tel.: +886 3 5712121x54248; fax: +886 3 5733722.
E-mail address: karshe.ee92g@nctu.edu.tw (H.S. Ling).

1350-4495/$ - see front matter © 2009 Elsevier B.V. All rights reserved.
doi:10.1016/j.infrared.2009.05.026

operations, shows much better performance at higher temperatures.

2. Experiments

Four QDIP samples were used in this study. They were prepared by a Veeco GEN-II molecular beam epitaxy system on (0 0 1) semi-insulating GaAs substrates. Each sample contained ten layers of QDs separated by GaAs barrier layers as the active region, which was then sandwiched between two 500 nm n^{+}GaAs contact layers. A surface QD layer with the same growth condition as the imbedded QD layers was also deposited for AFM measurement. The first two samples were prepared to compare the confinement-enhanced DWELL (CE-DWELL) structure (sample A) with the conventional DWELL structure (sample B). In both samples the GaAs barrier layers are 51 nm. For the CE-DWELL structure, 2.2 MLs of InAs QDs were deposited on a 2 nm $In_{0.15}Ga_{0.85}As$ layer and then followed by a 2.5 nm $Al_{0.3}Ga_{0.7}As$ confinement layer and a 4.5 nm $In_{0.15}Ga_{0.85}As$ well layer. As for the conventional DWELL sample, the $Al_{0.3}Ga_{0.7}As$ layer was replaced by $In_{0.15}Ga_{0.85}As$ while all other growth parameters were kept the same. Similar QD densities were shown in both samples to be about $2.1 \times 10^{10}\ cm^{-2}$. The other two samples were grown to investigate the CE-DWELL structures with thin AlGaAs layers (sample C) and thick AlGaAs layers (sample D). Compared with the previous two samples, thicker GaAs barrier layers (72 nm) were purposely grown. The thicker GaAs barriers can provide longer acceleration path for conductive carriers to enhance the current gain and thereby the responsivity [3]. Besides, the strain energy accumulated in the active region due to In(Ga)As layers is reduced which is favorable for a better epitaxial quality. 2.4 MLs of InAs QDs were deposited on a 2 nm $In_{0.15}Ga_{0.85}As$ layer and covered by $Al_{0.3}Ga_{0.7}As/In_{0.15}Ga_{0.85}As$ structure to comprise the CE-DWELL unit. The total thickness of the CE-DWELL structure was kept at 8 nm. For sample C, 2 nm of $Al_{0.3}Ga_{0.7}As$ confinement enhancing layer was used, while the deposition thickness of the $Al_{0.3}Ga_{0.7}As$ layer is 3 nm in sample D. The QD densities in sample C and D were determined by AFM to be around $2.6 \times 10^{10}\ cm^{-2}$, which was slightly higher than that in sample A and B due to the increased InAs MLs. On the other hand, the dot sizes determined by the AFM scan were similar for all the samples with the height about 13–17 nm and the base length about 40–55 nm. The schematic of the CE-DWELL sample structure and the device parameter differences in sample A–D are shown in Fig. 1.

Due to the strain distribution, the deposited thin $Al_{0.3}Ga_{0.7}As$ layer was expected to aggregate in areas without QDs first. Such a property is favored since with a proper AlGaAs thickness the structure can provide barriers that enhance the confinement in the lateral direction but do not deteriorate the carrier transport through QDs in the vertical direction much. In order to confirm this, the active layer structure of sample A was examined by the cross-sectional TEM image shown in Fig. 2. It is clearly seen that the AlGaAs layer is flat instead of conforming to the shape of the InAs QDs. The confinement effect of the AlGaAs layer was then verified with the photoluminescence (PL) measurement. At 77 K, the ground state energy measured for sample A, B, C and D is 1.090 eV, 1.028 eV, 1.092 eV and 1.119 eV respectively. Compared with sample B, the inserted AlGaAs layers in other samples induce enhanced confinement effect and therefore cause a blueshift for the ground state energy. Such an enhancement in confinement effect is even stronger with thicker AlGaAs layers, so the ground state energy of sample D is 27 meV higher than that of sample C. We attribute the observed blueshift to arise from the enhanced confinement effect of the QDs rather than the composition change of the dots which might result from different capped materials, for it has been reported that capping the InAs QDs with an Al contained layer should instead cause a redshift for the ground state energy due to the suppression of the In segregation [12].

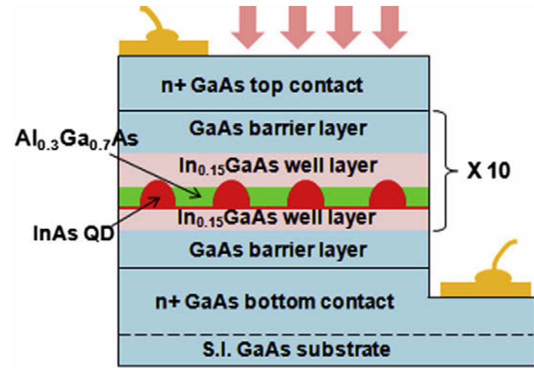

	sample A	sample B	sample C	sample D
GaAs barrier	51 nm	51 nm	72 nm	72 nm
top InGaAs	4.5 nm	7 nm	4 nm	3 nm
AlGaAs	2.5 nm	-	2 nm	3 nm
InAs	2.2 MLs	2.2 MLs	2.4 MLs	2.4 MLs

Fig. 1. The schematic diagram of the CE-DWELL QDIPs and the comparison of device parameters between samples.

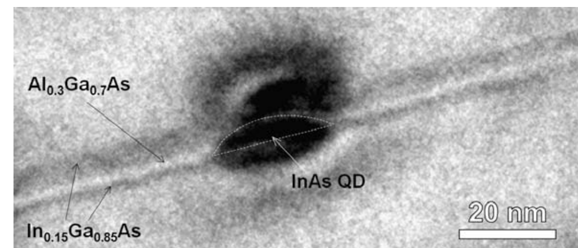

Fig. 2. The cross-sectional TEM image of the CE-DWELL structure.

Standard processing techniques were then applied for the device fabrication. $260 \times 370\ \mu m^2$ mesas with AuGe contact rings were formed to allow normal incidence measurement from the mesa top. In all measurements, the bottom contact is referred as ground. The photocurrent spectra were measured by a Fourier transform infrared spectrometer and the absolute responsivity was calibrated by a 1273 K blackbody radiation source with lock-in techniques. A Ge wafer was inserted in the optical path to filter out photons with wavelength shorter than 2 μm. While the optical properties of the device at different temperatures were measured using a close cycled helium cryostat, the dark I–V characteristic and the noise level of the device at different temperatures were obtained with a liquid helium dewar. The noise spectrum was measured by feeding the amplified dark current into a fast Fourier transform spectrum analyzer.

3. Results and discussion

3.1. Comparison between the confinement-enhanced DWELL and the conventional DWELL

Fig. 3 shows the photocurrent spectra and the bias dependent responsivity curves for sample A and sample B at 77 K. The peak wavelength of the CE-DWELL device (sample A) is around 8 μm which is shorter than that of the conventional DEWLL device (9.2 μm in sample B) as expected from the enhanced confinement

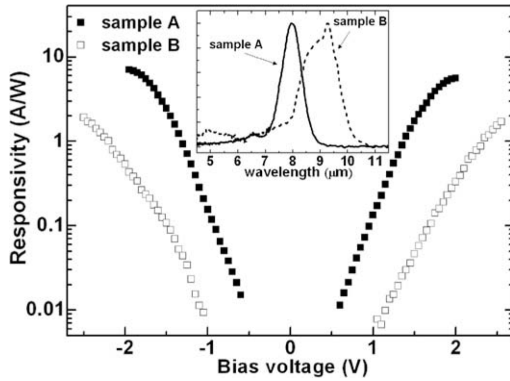

Fig. 3. The voltage dependence of the peak responsivity of the two samples at 77 K. The insert shows the responsivity spectra of the two samples at −1 V and 77 K.

effect due to the inserted AlGaAs wide bandgap layers. The relatively narrow bandwidth ($\Delta\lambda/\lambda_p < 15\%$) of the spectrum suggests that bound to bound transitions in the QDs are responsible for the infrared absorption in sample. Comparing the responsivity curves of the two samples, a clear increase of the responsivity in sample A is shown over the whole bias region. The enhanced quantum confinement greatly increases the responsivity of the device as expected. At −1.2 V and 77 K, the responsivity for sample A is 0.54 A/W while it is only 0.023 A/W for sample B with the conventional DWELL structure.

To further probe the origin of the increase of responsivity, the device current gain was calculated assuming the G-R noise dominates, and the quantum efficiency was then separated from the responsivity [13]. Both the current gain and the quantum efficiency are shown in Fig. 4 for comparison. The difference in responsivity is primarily attributed to the difference of quantum efficiency. Compared with the quantum efficiency of sample B, the quantum efficiency of sample A is much higher over the measured bias range and increases faster with the applied voltage. The highest quantum efficiency in sample A is around 2% at −1 V, which is clearly superior to that in sample B (0.08% at −1.3 V). The inserted AlGaAs layer confines the QD's excited state wavefunction to be more localized, so the absorption strength of the ground state electrons is enhanced due to the better wavefunction coupling. In addition, the excited state energy in sample A is estimated to be ~60 meV higher than that in sample B from the PL and photocurrent spectra. The escape probability is thus higher and as a result the operation voltage is lower for sample A with the confinement-enhanced structure. On the other hand, the two samples have essentially similar current gain in the bias region of −1.3 to 1.25 V, so the carrier transport property is preserved in the CE-DWELL structure even though the wide bandgap AlGaAs layer was added. This is partly due to the reduced InGaAs thickness and also because the AlGaAs layer has such a thin thickness that the upper portion of the QD is left uncovered to the flow path of carriers.

The higher ground state energy of the CE-DWELL sample could generate higher dark current and it has been observed in the measurement. The dark current density was 3.8×10^{-4} A/cm^{-2} at −1 V at 77 K for sample A but it was only 3.3×10^{-5} A/cm^{-2} for sample B under the same conditions. However, the increase of the quantum efficiency overcomes the increased dark current. As a result, the overall performance of CE-DWELL QDIPs is far more superior to that of the conventional ones. At 77 K, the highest detectivity measured for sample A is 1×10^{10} cm Hz$^{0.5}$/W (at −0.9 V), which is ten times higher than that in sample B (1×10^{9} cm Hz$^{0.5}$/W at −1.2 V).

3.2. Comparison of the CE-DWELL QDIPs with thin and thick AlGaAs layers

Fig. 5 shows the photocurrent spectra of sample C and sample D as well as the bias dependent responsivity curves at 77 K and 200 K. Both CE-DWELL samples reveal suitable response band for LWIR detection. The response peak of sample C is at 8.2 μm, while that of sample D is slightly shorter, at about 8 μm. The thicker AlGaAs layer in sample D pushed the response peak toward short wavelength as expected. Again, both of the spectra show small relative bandwidths ($\Delta\lambda/\lambda_p$) of about 10% with the bound to bound transitions. Comparing the responsivity of the two samples, sample C shows higher reponsivity at both temperatures. At 200 K, it reaches 0.37 A/W at 0.8 V. Although there is a stronger confinement effect in sample D, because of thicker AlGaAs layers, the responsivity instead degraded. However, the responsivity of sample D (37 m A/W at −1.6 V at 77 K) is still higher than that of the sample without AlGaAs layers (23 m A/W for sample B under the same electric field, i.e. −1.2 V).

To understand the origin of the inferior responsivity in the thick AlGaAs device, the comparison of current gain for sample C and sample D at 77 K and 200 K is shown in Fig. 6. Clear degradation of current gain is shown in sample D due to the thicker AlGaAs layers. Furthermore, the two samples show distinct gain behaviors. The current gain of sample D possesses a clear asymmetry between the positive bias and the negative bias. Because of thicker AlGaAs layers used, the quantum dots in sample D are virtually covered. When positively biased, the photo-generated electrons have to overcome the potential barrier of AlGaAs and pass through the InGaAs well. The capture probability of the excited carriers into

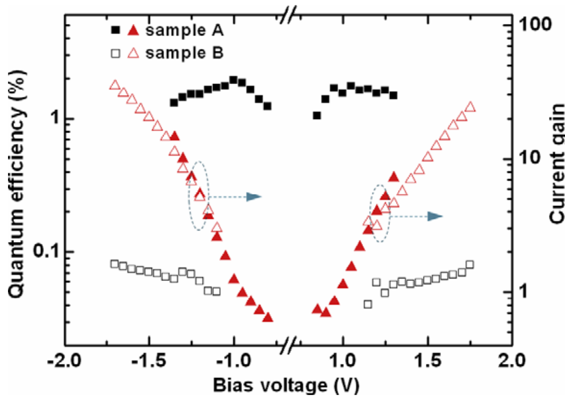

Fig. 4. The quantum efficiency (squares) and current gain (triangles) curves of the two samples at 77 K.

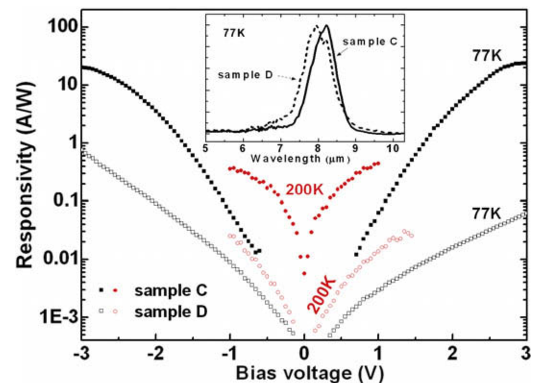

Fig. 5. The voltage dependence of the peak responsivity of the two samples at 77 K and 200 K. The insert shows the responsivity spectra of the two samples at −1.35 V and 77 K.

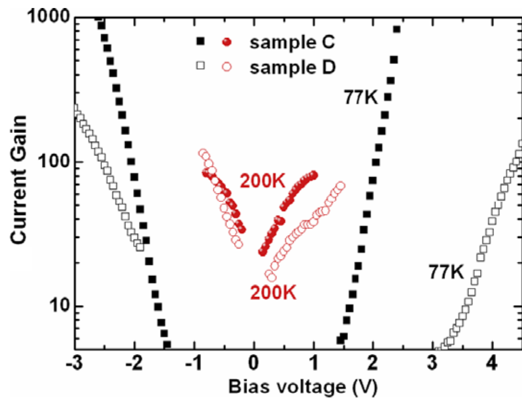

Fig. 6. The current gain curves of the two samples at 77 K and 200 K.

the adjacent InGaAs well is high when the bias is low. Higher positive voltages are needed to reach the same current gain as that in the reverse bias. On the other hand, in sample C, because of thinner AlGaAs layers, the current gain is more symmetric under different bias polarities and it has a much higher gain than that of sample D under the same positive bias. The current gain difference of the two samples also depends on the device temperature. At higher temperatures, because of the additional thermal energy, the capture probability of electrons decreases in both bias polarities. The gain increases in both samples and the asymmetry reduces in sample D. By the way, the current gain of sample C (3.7 at -15 kV/cm at 77 K) is higher than that of sample A (1.2 at -15 kV/cm at 77 K) as expected, showing the advantage of thicker GaAs barrier for QDIPs.

The AlGaAs layer in sample D, although is too thick from the responsivity point of view, is effective to reduce the dark current. This is especially true at high temperatures and low bias voltages. The dark current density for sample D (thick AlGaAs) and sample C (thin AlGaAs) are 1.4×10^{-8} A/cm^2 and 4.1×10^{-6} A/cm^2 respectively at -1 V and 77 K. The AlGaAs layers in sample D effectively block the low energy part of the dark current, so the detectivity of sample D is not necessarily worse than that of sample C. Fig. 7 shows the specific detectivity of the two samples at different temperatures. At 77 K, the highest measured detectivity for sample C is 3.6×10^{10} cm Hz$^{0.5}$/W at 1.4 V. This shows the superior performance of the CE-DWELL structure. However, as the temperature increases, sample D starts to show better performance. At 220 K, the highest detectivity measured for sample D is 4.85×10^7 cm Hz$^{0.5}$/W at -0.15 V, which is about 2.4 times higher than that of sample C. When the temperature is further raised to 240 K, the detectivity reaches 1.4×10^7 cm Hz$^{0.5}$/W at -0.1 V for sample D, while for sample C the dark current is too high for the measurement. Moreover, the BLIP temperature for sample D is about 140 K within ±0.3 V which is 40 K higher than that of sample C.

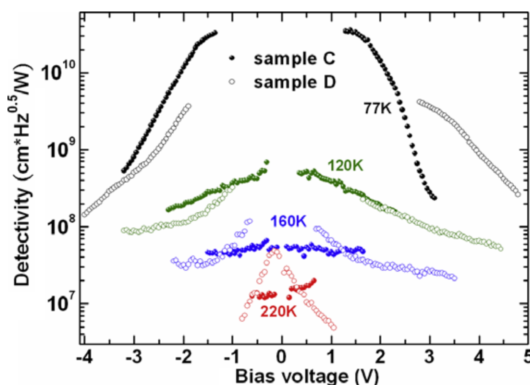

Fig. 7. The specific detectivity curves of the two samples at 77 K, 120 K, 160 K and 220 K.

The comparison of sample C and sample D shows an important factor for the high temperature operation. Sample C is a typical high performance detector at 77 K with good carrier collection capability. However, as the temperature increases, the superior carrier transport property induces high dark current which is not acceptable in real applications. On the other hand, although the insertion of the thicker AlGaAs layer in sample D degrades the responsivity, the dark current is suppressed even more especially at small biases. As the temperature increases, the thermal energy helps the photocarrier collection and provides a better performance at higher temperatures. This indicates the importance of the current suppression for the high operating temperature devices.

4. Summary

We designed a confinement-enhanced DWELL (CE-DWELL) structure for QDIPs. With this new design, LWIR QDIPs with operation temperatures higher than 200 K were demonstrated. A thin AlGaAs layer was inserted on top of the InAs QDs in the DWELL structure as the confinement enhancing layer. This enhanced confinement effect greatly enhanced both the absorption quantum efficiency and the escape probability. At 77 K, the maximal quantum efficiency was increased by about 25 times and the specific detectivity was increased by about 10 times with a lower bias voltage. Two different CE-DWELL structures were further studied. With proper device parameters, both LWIR CE-DWELL QDIPs achieve high temperature operations despite the dramatic differences in their device characteristics. The device with better performance at lower temperatures does not necessarily have better performance at elevated temperatures. Better suppression of the dark current is the key to the high temperature operation QDIPs.

Acknowledgement

This work was supported by the National Science Council under contract number NSC96-2221-E009-211-MY3.

References

[1] J. Urayama, T.B. Norris, J. Singh, P. Bhattacharya, Phys. Rev. Lett. 86 (2001) 4930–4933.
[2] L. Jiang, S.S. Li, N.T. Yeh, J.I. Chyi, C.E. Ross, K.S. Jones, Appl. Phys. Lett. 82 (2003) 1986–1988.
[3] S. Chakrabarti, A.D. Stiff-Roberts, P. Bhattacharya, S. Gunapala, S. Bandara, S.B. Rafol, S.W. Kennerly, IEEE Photon. Tech. Lett. 16 (2004) 1361–1363.
[4] P. Bhattacharya, X.H. Su, S. Chakrabarti, G. Ariyawansa, A.G.U. Perera, Appl. Phys. Lett. 86 (2005) 191106.
[5] H. Lim, S. Tsao, W. Zhang, M. Razeghia, Appl. Phys. Lett. 90 (2007) 131112.
[6] E.T. Kim, Z. Chen, A. Madhukar, Appl. Phys. Lett. 79 (2001) 3341–3343.
[7] S. Raghavan, D. Forman, P. Hill, N.R. Weisse-Bernstein, G. Von Winckel, P. Rotella, S. Krishna, S.W. Kennerly, J.W. Little, J. Appl. Phys. 96 (2004) 1036–1039.
[8] X. Lu, J. Vaillancourt, M.J. Meisner, A. Stintz, J. Phys. D 40 (2007) 5878–5882.
[9] R.S. Attaluri, J. Shao, K.T. Posani, S.J. Lee, J.S. Brown, A. Stintz, S. Krishna, J. Vac. Sci. Technol. B 25 (2007) 1186–1190.
[10] R.V. Shenoi, R.S. Attaluri, A. Siroya, J. Shao, Y.D. Sharma, A. Stintz, T.E. Vandervelde, S. Krishna, J. Vac. Sci. Technol. B 26 (2008) 1136–1139.
[11] S.D. Gunapala, S.V. Bandara, C.J. Hill, D.Z. Ting, J.K. Liu, S.B. Rafol, E.R. Blazejewski, J.M. Mumolo, S.A. Keo, S. Krishna, Y.C. Chang, C.A. Shott, IEEE J. Quantum Elect. 43 (2007) 230–237.
[12] Z.Y. Zhang, B. Xu, P. Jin, X.Q. Meng, Ch.M. Li, X.L. Ye, Z.G. Wang, J. Appl. Phys. 92 (2002) 511–514.
[13] S.Y. Wang, M.C. Lo, H.Y. Hsiao, H.S. Ling, C.P. Lee, Infrared Phys. Technol. 50 (2007) 166–170.